

Effect of viscosity on a well-posed one-dimensional two-fluid model for wavy two-phase flow beyond the Kelvin-Helmholtz instability: limit cycles and chaos

Martín Lopez de Bertodano¹ and William D. Fullmer²

¹ School of Nuclear Engineering, Purdue University, West Lafayette, IN 47907, USA

² Department of Chemical and Biological Engineering, U. of Colorado, Boulder, CO 80309
bertodan@purdue.edu, william.fullmer@colorado.edu

Abstract

The one-dimensional (1D) Euler formulation of the Two-Fluid Model (TFM) becomes ill-posed by the Kelvin-Helmholtz (KH) instability which is not present in the 1D Euler equations of single phase flow, though it is present in the multidimensional equations where the single phase flow problem is also ill-posed. It is well known that the 1D TFM may be rendered well posed by including appropriate short wave physics, i.e., by making it more complete. In the case of near horizontal stratified flow, surface tension is the appropriate force which restores the KH force at short wavelengths. A linear stability analysis shows that the model is well-posed, but that material waves grow at a finite rate beyond a critical wavelength. Upon further nonlinear development the wave fronts become steep in a similar fashion to Shallow Water Theory waves and the 1D TFM is bounded by viscosity due to dissipation in shock like structures.

A 1D TFM numerical simulation of near horizontal stratified two-phase flow is performed where the TFM, including surface tension and viscous stresses, is simplified to a two-equation model using the fixed flux approximation. As the angle of inclination of the channel is increased, i.e., increasing the body force to drive the flow, the flow becomes KH unstable and waves appear that develop steep fronts. It is shown that these waves grow until they reach a limit cycle due to viscous dissipation. Upon further inclination of the channel, chaos is observed. The appearance of chaos in a 1D TFM implies a nonlinear process equivalent to the Kolmogorov's turbulent cascade that transfers energy intermittently from long wavelengths where energy is produced to short wavelengths where energy is dissipated by viscosity, so that an averaged energy equilibrium in frequency space is attained.

Boundedness is a necessary condition for a chaotic TFM, i.e., a nonlinearly well behaved model, but the more restrictive hyperbolic condition of the Euler formulation of the 1D TFM, i.e., zero wave growth at all wavelengths, is not necessary. In other words, it is not necessary to remove the KH instability to have a well behaved TFM.

Keywords: Two-fluid model, well-posedness, Kelvin-Helmholtz instability, nonlinear, chaos

Introduction

It is well known that the one-dimensional two-fluid model (1D TFM) may become well-posed once appropriate short wavelength physics is incorporated. For example the surface tension force makes the TFM well-posed for horizontal stratified flows beyond the Kelvin-Helmholtz (KH) instability [1]. This is a proper solution to the linear stability problem, but the TFM is inherently non-linear, and most questions about the non-linear stability remain largely unanswered. The purpose of this paper is to investigate one case of 1D TFM non-linear KH stability.

The state-of-the-art of the 1D TFM stability analysis remains more or less where it was when the present generation of US TFM nuclear reactor safety codes were written in the early seventies, that is linear stability theory. Shortly afterward the field of non-linear dynamics and chaos experienced a boom that has not transcended yet into the understanding of the stability of the TFM.

In the first place Whitham [2] elaborated a set on non-linear solutions to the two equation shallow water theory (SWT) consisting of shocks and expansion waves and identified the kinematic SWT instability. But SWT does not resemble the TFM in one important aspect, it does not include the dynamic KH instability which is stronger.

Kreiss and Ystrom [3] (KY) analysed a two-equation model that is similar to the TFM beyond the KH instability. They obtained nonlinear material shocks and expansion waves similar to SWT and observed that the interaction of viscosity with the material shocks limits the growth of the waves. Furthermore, Fullmer et al. [4] showed that the KY equations are chaotic.

Recently Lopez de Bertodano et al. [5] derived a two equation TFM that reduces exactly to SWT for flow conditions below the KH instability, thus rendering the results of Whitham[2] applicable to TFM analysis. Furthermore the model resembles the KY equation for flow conditions beyond the KH instability. It is important to clarify that all the two-equation models mentioned are based on the fixed flux assumption which allows local instabilities like SWT and KH but precludes global instabilities like flow excursion and density waves. The counterpart is the drift-flux model which does the opposite. Of course the full TFM includes both local and global instabilities.

In this paper we apply the two-equation TFM of Lopez de Bertodano et al. [5] obtained from the full TFM of Fullmer et al. (2014b) developed for the experiment of Thorpe [6] to perform a stability assessment that includes linear analysis, nonlinear simulations of limit cycles and chaos. The focus is on the interaction of viscosity with nonlinear wave development, which increases the viscous dissipation.

Two Equation model

The incompressible two-equation TFM for near horizontal stratified flow, Fig. 1, of Lopez de Bertodano et al. [5] is,

$$\frac{\partial \alpha_1}{\partial t} + u_1 \frac{\partial \alpha_1}{\partial x} + \alpha_1 \frac{\partial u_1}{\partial x} = 0 \quad (1)$$

$$\begin{aligned} \frac{\partial u_1}{\partial t} + \frac{1 - \alpha_1}{\alpha_1 + r(1 - \alpha_1)} \left(u_1 + r \frac{\alpha_1}{1 - \alpha_1} (2u_2 - u_1) \right) \frac{\partial u_1}{\partial x} - \frac{1 - \alpha_1}{\alpha_1 + r(1 - \alpha_1)} C \frac{\partial \alpha_1}{\partial x} \\ = \frac{1 - \alpha_1}{\alpha_1 + r(1 - \alpha_1)} \left(v \frac{\partial^2 u_1}{\partial x^2} + \frac{\sigma H}{\rho_1} \frac{\partial^3 \alpha_1}{\partial x^3} + F \right) \end{aligned} \quad (2)$$

where,

$$C = \left[r \frac{(u_2 - u_1)^2}{1 - \alpha_1} - g_y H \right] \quad (3)$$

and

$$F = g_x - \frac{1}{\alpha_1 H} \frac{f_1}{2} u_1^2 + \frac{1}{\alpha_2 H} \frac{f_2}{2} r u_2^2 + \left(\frac{1}{\alpha_1 H} + \frac{1}{\alpha_2 H} \right) \frac{f_i}{2} r (u_2 - u_1)^2 \quad (4)$$

Two more equations are needed for closure. The first is the void fraction condition

$$\alpha_1 + \alpha_2 = 1 \quad (5)$$

and the second is the fixed flux condition obtained from the time derivative of the void fraction condition combined with the continuity equations:

$$\frac{\partial}{\partial t} (\alpha_1 + \alpha_2) + \frac{\partial}{\partial x} (\alpha_1 u_1 + \alpha_2 u_2) = 0 \rightarrow \alpha_1 u_1 + \alpha_2 u_2 = j_1 + j_2 = j \quad (6)$$

where j is the total volume flux which is uniform, i.e., $j(x, t) = j(t)$, for isothermal adiabatic incompressible flow and in most experiments it is close to steady. This key assumption greatly simplifies the equations without removing the local material instabilities.

If C is negative and surface tension is neglected the two equation model becomes the well-known 1D SWT equations [2], [7]. Furthermore $C = 0$ is the long wavelength Kelvin-Helmholtz criterion,

$$(u_2 - u_1)^2 > \frac{1 - \alpha_1}{r} (1 - r) g_y H \quad (7)$$

Therefore if C is positive the equations represent the Kelvin-Helmholtz unstable regime which is a case of the TFM that is beyond the scope of SWT. We are now in a position to define the types of waves and instabilities that will be analysed.

The dynamic wave speed, derived later, is given by $c = \sqrt{-\alpha_1 C}$ and the corresponding instability condition is $C > 0$, associated with the dynamic KH instability. Because of the analogy between the TFM and SWT it may be stated that the linear and non-linear behaviour of the dynamically stable TFM (i.e., $C < 0$) may be understood in terms of many well-known results for SWT. If $C = 0$ and $F = 0$ the system becomes the water faucet model of Ransom [8] which is of practical interest to the verification of the TFM for nuclear reactor safety codes.

The case $C > 0$ corresponds to the dynamically unstable incompressible TFM and is of unique interest to two-phase flow analysis in general and reactor safety codes in particular because it is the ill-posed criterion, when surface tension is not included. However it has not been explored beyond the pioneering mathematical analyses of Kreiss and Yström[3].

Viscous term

Additional constitutive equations are required for the closure of the wall and interfacial shear terms and the effective viscosities. For the present calculations the values are $f_1 = f_2 = 0.005, f_i = 0.014$.

More importantly, the effective viscosity needs to be specified. At this point, a complete model for the turbulent viscosity is not available. A very rough, order-of-magnitude model is proposed, which we believe suffices for the numerical experiments herein. Since the densities of the Thorpe experiment [6] are quite close, a first order approximation is to neglect the damping action of the interface and treat the two-fluid flow as a single phase mixing layer, which can be derived analytically [9],

$$\nu_T = 0.3902^2 \cdot S \cdot \delta(t) \cdot \Delta U, \quad (8)$$

where S is the spreading rate, δ is the mixing layer thickness and ΔU is the velocity difference between the two streams. The derivation of Eq. (9) is made by assuming the mixing layer is self-similar. Therefore Eq. (9) is only valid if $S \equiv \frac{1}{\Delta U} \frac{d\delta}{dt}$ is a constant; which is the case for single phase flow. With the Thorpe problem the velocities and hence the difference are accelerating linearly so that Eq. (9) holds only if the mixing layer thickness expands quadratically in time. A 2-D VOF simulation performed previously by Fullmer et al. [10] was used to verify that this is approximately the case and $S \approx 0.0137$ to 0.0252 . Finally, rather than using a time dependent mixing layer thickness, the maximum value is taken, i.e., $\delta(t) \approx H$. This results in the very simple turbulent viscosity model which is used for all numerical simulations,

$$\nu_T = 0.003 \cdot H \cdot |u_R|. \quad (9)$$

Thorpe Experiment

The conditions and properties of the Thorpe experiment [9] will be used for the linear and nonlinear stability analyses that follow. The measured critical wavelength data for the inclination angle $\sin(\theta) = 0.072$ rad will also be used to compare with the linear stability analysis. In the experiment two immiscible liquids, water and a kerosene - carbon tetrachloride mixture, equally fill a rectangular channel of dimensions 0.03 m tall, 0.1 m wide and 1.83 m long. The material properties are given in Table 1.

Table 1: Material properties of the Thorpe experiment.

Property	Water	Kerosene
ρ_k (kg/m ³)	1000	780
μ_k (Pa s)	0.001	0.0015
σ_{12} (N/m)	0.04	-

Initially the channel is at rest in the horizontal position allowing the fluids to a complete uniform equilibrium. Then the channel is suddenly tilted at a small specified angle and a counter-current flow is developed as the denser water rushes down pushing the lighter kerosene up. For the case $\sin(\theta) = 0.072$ a series of photographs of the flow viewed from the side were published. The dominant wavelength measured at the onset is approximately 3.5 ± 1 cm.

Linear stability

First we consider the model with $F = 0$. Eqs. (1) and (2) can be written as:

$$\mathbf{A} \frac{\partial}{\partial t} \underline{\phi} + \mathbf{B} \frac{\partial}{\partial x} \underline{\phi} + \mathbf{D} \frac{\partial^2}{\partial x^2} \underline{\phi} + \mathbf{E}' \frac{\partial^3}{\partial x^3} \underline{\phi} = 0 \quad (10)$$

The matrices \mathbf{D} and \mathbf{E}' , which include the physical viscous and surface tension terms in the momentum equation, are usually not included in a 1D TFM.

The characteristics, given by the condition $\text{Det}[\mathbf{B} - \lambda \mathbf{A}] = 0$ describe the behaviour of the first order system:

$$\begin{aligned} C < 0: \lambda &= u_1 \pm \sqrt{|C|\alpha_1}, & \text{two real roots} \\ C = 0: &= u_1, & \text{one real root} \\ C > 0: &= u_1 \pm i\sqrt{|C|\alpha_1}, & \text{two imaginary roots} \end{aligned}$$

The first two cases are well-posed and well-understood. However the last case leads to difficulties and will be analysed in detail using a dispersion analysis.

The dispersion relation extends the results of the characteristic analysis to the full spectrum of wavelengths and includes the effects of viscosity and surface tension. The first step is to linearize the two equation system using $\underline{\phi} = \underline{\phi}_0 + \underline{\phi}'$. Then a Fourier solution, $\underline{\phi}' = \hat{\phi}' e^{i(kx - \omega t)}$, is applied to the linearized equations, where k and ω are the wave number and the angular frequency. The solution for a non-trivial perturbation must satisfy:

$$\text{Det}[-i\omega \mathbf{A} + ik \mathbf{B} + (ik)^2 \mathbf{D} + (ik)^3 \mathbf{E}'] = 0 \quad (11)$$

Stable model

The stable model (i.e., $C \leq 0$) corresponds to gas velocities below the KH limit. The wave speeds in the limit of infinitesimal wavelengths (i.e., $k \rightarrow \infty$) are the characteristic speeds, which are real so the stable model is hyperbolic. Hyperbolicity is a characteristic feature of well-posed stable wave propagation models. Stable waves do not grow, and they propagate at the characteristic speed. The inviscid case without surface tension is the well-known SWT [2]. While the linear stability characteristics are very simple, the nonlinear behaviour is not so simple and leads to material shocks equivalent to Burgers' equation.

The results for finite wavelengths retain this characteristic behavior, but the effects of viscosity and surface tension make the system dissipative (i.e., the wave amplitude decreases with time) and dispersive (i.e., different wavelengths travel at different speeds) respectively.

Unstable model

The fixed flux TFM approximation is unique, compared with SWT, because it becomes dynamically unstable once the KH condition, Eq. (7), is reached. The dispersion analyses including artificial "void" viscosity, kinematic viscosity and surface tension is performed with the conditions of the experiment of Thorpe: $H = 0.03 \text{ m}$, $\alpha = 0.5$, $u_1 = -u_2 = 0.2 \frac{\text{m}}{\text{s}}$, $r = 0.78$, $\nu = 0.0001 \text{ m}^2/\text{s}$ and $\frac{\sigma H}{\rho_1} = 1.2 \times 10^{-6} \frac{\text{m}^4}{\text{s}^2}$ are shown in Fig. 2. The value of the kinematic viscosity, was obtained by Fullmer et al. [10] with Eq. (9) multiplied by a covariance factor, to account for the vorticity missing in a 1D model, to obtain the right amount of viscous dissipation.

The first significant result is the fast wave growth rate for all cases because the KH condition is exceeded. The basic, or fundamental, 1D TFM dispersion relation is obtained from the solution to Eq. (11) by setting $\varepsilon = \nu = 0$ and $\sigma = 0$. Beyond the KH limit this model is ill-posed, i.e., growth rates increase unboundedly as the wavelength shrinks to zero. The zero wavelength growth rate is infinite for any relative velocity except for the trivial case of homogeneous flow (i.e., zero relative velocity). This is the well-known ill-posed TFM [11]. Furthermore, when wall and interfacial friction are included, even with unrealistically large coefficients values, they do not change the ill-posed nature of the dynamic instability at the zero wavelength. Adding kinematic viscosity, $\nu = 0.0001 \text{ m}^2/\text{s}$, makes the model well-posed since the growth rate is finite at zero wavelength but it is still maximum there, $\omega_i = \frac{\alpha_1 C}{\nu}$, which is unphysical. This well-known result is not rigorously ill-posed but it is practically the same. On the other hand, Fig. 2 shows that surface tension makes the model well-posed with the advantage that it is more realistic. The cut-off wavelength corresponding to the surface tension of water, i.e., $\sigma = 0.04 \text{ N/m}$, is now approximately 10 mm. Furthermore the most dangerous wavelength matches approximately the experimental measurement of 35 mm. This confirms that for the Thorpe experiment [9] the KH instability is indeed appropriate. Surface tension regularization [1] is the earliest published demonstration that the TFM may be rendered well-posed for unstable flow by including appropriate short wavelength physics. The significance of this simple example

is that the TFM is ill-posed only because it is incomplete. Nevertheless, even when the model is well-posed, there is unlimited wave growth unless some nonlinear stability mechanism is available.

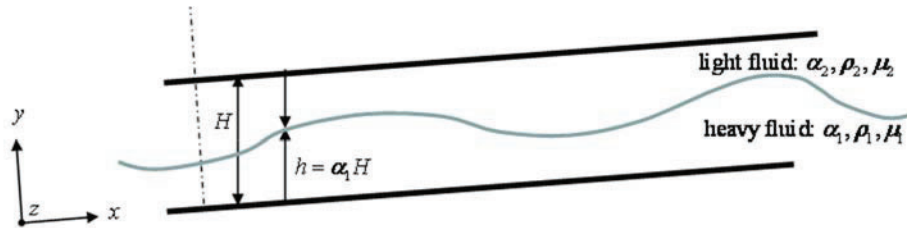


Figure 1

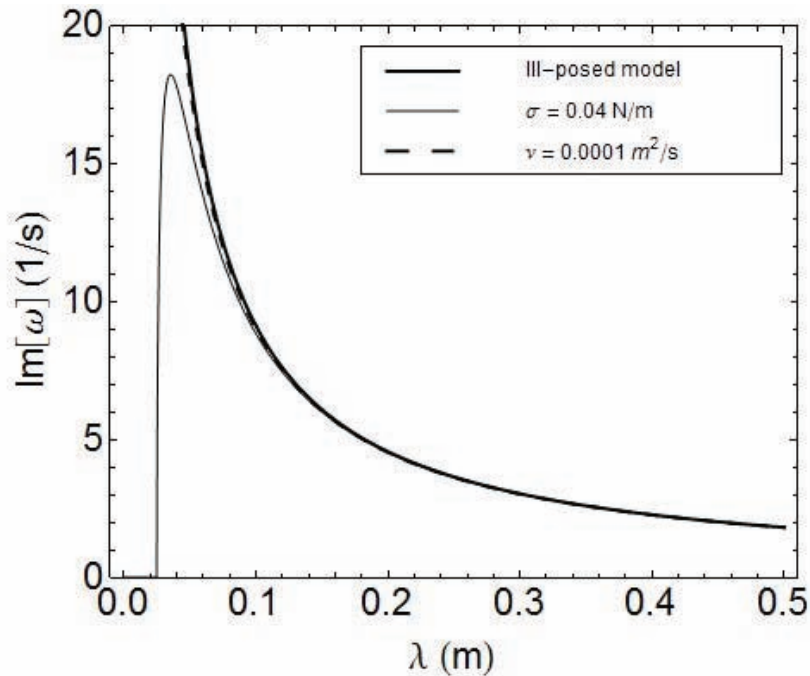


Figure 2

Nonlinear Stability

In this section the nonlinear analysis is achieved with numerical simulation. The 1-D model of Eqs. (1) and (2) is solved numerically with *Mathematica*. The primary objective of the nonlinear analysis is to understand how a model that is linearly unstable behaves in the long term. Barnea and Taitel [12] have shown that, in general, when the governing model is linearly unstable, perturbations grow, cut-off and critical wavelengths are generally consistent with linear theory. The typical initial nonlinear behavior is for waves to steepen into Burgers-like shocks [2]. Furthermore, Kreiss and Ystrom [3] have demonstrated that the waves stop growing because of

the effect of viscosity at the material shocks. Here, we seek to understand what happens as $t \rightarrow \infty$.

Unfortunately the time and space constraints of the Thorpe problem make it impossible to do such a calculation for a physical system. In order to run a simulation for a long period of time, a problem is proposed to mimic the conditions in the center of the channel of the Thorpe problem but in an infinite domain, i.e., with periodic boundary conditions at each end. An angle of inclination greater than $\theta = 0.027 \text{ rad}$ is required for the KH critical velocity. The channel is assumed to be horizontal and of the same geometry as the Thorpe channel. The length of the channel is selected to be $L = 1 \text{ m}$. It was found that starting the simulations from the equilibrium condition with an initial perturbation in the void fraction helped reduce unnecessary transients.

To keep the flows from being brought to rest under the dissipative shear models, a constant, uniform source must be added. In the physical case, the axial component of gravity acts in the same direction for both fluids. But if it were not for the closed ends, both fluids would accelerate downward and reach larger phasic velocities than in the countercurrent case. To keep the flow countercurrent, a horizontal force (x-direction) will be added to each phase. The additional source term for Eq. (4) is $F_h = (1 - r)g \sin \theta$. The initial condition is $\alpha_1 + 0.02 e^{\left(\frac{x-x_0}{0.01}\right)^2}$ and the velocity is set by the kinematic condition, $F = 0$.

Three cases are shown in Figs. 3 and 4 for angles $\theta = 0.0272, 0.0274, 0.028 \text{ rad}$. In order to view the long term dynamics of the problem, a phase space is constructed. Ideally, the two state variables could be used at a single location. However, due to the constant flux condition, this produces a tight phase-space projection which makes it difficult to distinguish one type of trajectory from another. (Consider if the rings of Saturn are viewed perfectly on edge, one cannot tell if they are just lines, or rings or some other type of two-dimensional structure.) Therefore a rather simple solution is taken here: the phase-space trajectory is constructed of the water void fraction at two locations about the center of the domain separated by 20 cm. For $\theta = 0.027 \text{ rad}$ and below, the model is asymptotically stable and these cases are not shown.

As the inclination and equilibrium velocity increase, the system no longer spirals into a singular equilibrium point but begins traveling around a ring in the phase space - this is a limit cycle. As the solution approaches the attractor, i.e., in this phase space representation at $\alpha(x = 0.4 \text{ m})$ vs $\alpha(x = 0.6 \text{ m})$ in Figs. 4a,b, the nonlinear stabilizing mechanisms balance with the long wavelength instability and a self-sustained wave is formed. This is an equilibrium solution because it remains stable as $t \rightarrow \infty$.

Figures 3a and 4a show the time evolution and limit cycle for $\theta = 0.0272 \text{ rad}$. Fig. 3a shows well defined waves with material shocks, as expected from the analysis of Whitham [2]. The frequency spectrum in Fig. 4a shows very few well defined frequencies.

As the inclination increases, the amplitude of the limit cycle grows and the waveform becomes more complex. Further increasing the inclination eventually leads to bifurcations. Figures 3b and 4b show the time evolution and limit cycle for $\theta = 0.0274 \text{ rad}$. The frequency spectrum now has several more well defined frequencies.

The exact route to chaos has not yet been fully explored and therefore it is not shown here, but Figures 3c, 4c show chaos for $\theta = 0.028 \text{ rad}$. The important result is that beyond the limit cycles, chaotic behavior develops, i.e., the attractor has developed into a strange attractor. The time trace in Fig. 3c shows that regular wave pattern is lost and seemingly random waves of different wavelengths and amplitudes take over. Furthermore the spectrum is now continuous as shown in Fig. 4c and exhibits the Kolmogorov slope, $-5/3$, over a segment.

The case of $\theta = 0.028 \text{ rad}$ is important for a few reasons. First, it shows that while the linear stability analysis predicts linear growth, the nonlinear behaviour is bounded. It is important to demonstrate this on a case that does not reach the physical limits of $\alpha_2 \in [0,1]$. It could be said that any model, even an ill-posed model, is bounded because of the physical limitations placed on the void fraction. However, this model is bounded by the attractor independent of physical limitations. Whether or not the level of instability is sufficient to cause regime transitions is another issue. Secondly, it is important simply to demonstrate that the 1-D two-fluid model is chaotic. While chaos in a fluid flow system is not new, it is interesting that this aspect of the multidimensional turbulent flow models is retained in the reduced 1-D TFM. The same cannot be said of the 1-D Navier-Stokes equations, i.e., turbulence does not develop naturally out of a 1-D single phase model. One implication of chaos in the unstable TFM is that simulations will be very sensitive to minor perturbations, even those resulting from differences in truncation error for different grids of the same problem. Therefore, convergence in the typical sense cannot be expected and another invariant must be sought, e.g., the turbulent energy spectrum.

Conclusions

The 1-D two-equation TFM for horizontal or slightly inclined two-phase flow, that results from the fixed flux assumption, has been used to dynamically simulate stratified wavy flow and its transition from smooth flow. The model is validated with the experimental data of Thorpe [6].

It was shown in Fig. 2 that the model with surface tension is well-posed and the linear stability analysis agrees well with the data of Thorpe for the dominant wavelength, validating the KH instability assumption. However the focus is on the nonlinear stability due to the interaction of viscosity with the nonlinear wave development which yields limit cycles and chaos. The path from limit cycles to chaos and the Kolmogorov spectrum shown in Fig 4 are strong indications that the 1D TFM is chaotic. Even though the Lyapunov coefficient has not yet been calculated for the TFM, the authors have already obtained a positive Lyapunov coefficient and the fractal dimension for a similar system of two equations by Kreiss-Ystrom [4].

For a narrow range of parameters, it is shown that the dynamics of the infinite domain problem are bounded by the attractor alone, independent of physical limitations, i.e., transition to regions of single-phase flow which are locally stable. The development of chaos is a consequence of a linearly unstable model. In some respects the development of chaos is advantageous: perturbations (errors) in solutions do not grow unboundedly, which may be suspected from linear stability alone. In other respects the appearance of chaos presents

additional challenges: any simulation that exhibits chaos in some space-time region must be run many times to determine the average behavior (as opposed to an artificially hyperbolic model).

Finally, chaos implies that a Kolmogorov nonlinear process applies to the 1D TFM, even though the mechanism of 1D material shocks is different from the 3D vortex turning and stretching of turbulence. Kolmogorov stability is a desirable alternative to the ill-posedness attributed to the 1D TFM in the past and there is no fundamental need to remove the KH instability with artificial mathematical devices, either differential or numerical, although this may be convenient in some engineering applications.

References

1. Ramshaw, J. D., and Trapp, J. A., 1978. "Characteristics, stability and short-wavelength phenomena in two-phase flow equation systems". *Nuclear Science and Engineering*, **66**, pp. 93–102.
2. Whitham, G.B., 1974. *Linear and Nonlinear Waves*, New York: Wiley, New York.
3. Kreiss, H.-O., and Yström, J., 2002. "Parabolic problems which are ill-posed in the zero dissipation limit," *Mathematical and Computer Modelling*, **35**, pp. 1271–1295.
4. Fullmer W. D. et al., 2014a. "Analysis of stability, verification and chaos with the Kreiss–Yström equations," *Applied Mathematics and Computation*, **248**, pp. 28-46.
5. Lopez de Bertodano, M. et al., 2013. "One-dimensional two equation two-fluid model stability," *Multiphase Science and Technology*, **25**.
6. Thorpe, J. A., 1969. "Experiments on the instability of stratified shear flow: immiscible fluids". *Journal of Mechanics*, **39**, pp. 25–48.
7. Wallis, G.B., 1969. *One-dimensional Two-phase Flow*, New York: McGraw-Hill, New York.
8. Ransom, V. H., 1984. Benchmark numerical tests, In: *Multiphase Science and Technology*, G. F. Hewitt, J. M. Delhay and N. Zuber eds., Hemisphere, Washington DC.
9. Pope, S. B., 2000. *Turbulent Flows*, first ed. Cambridge University Press, New York.
10. Fullmer, W. D., Lopez de Bertodano, M. A., and Ransom, V. H., 2011. "The Kelvin-Helmholtz instability: comparisons of one- and two-dimensional simulations," NURETH-14.
11. Lyczkowski, R. W., Gidaspow, D. and Solbrig, C. W., 1978. "Characteristics and stability analyses of transient one-dimensional two-phase flow equations and their finite difference approximations," *Nuclear Science and Engineering*, **66**, pp. 378-396.
12. Barnea, D., and Taitel, Y., 1994. "Non-linear interfacial instability of separated flow". *Chemical Engineering Science*, **49**, pp. 2341–2349.

Nomenclature

f	friction factor
g	acceleration due to gravity (ms^{-2})
H	channel height (m)
j	volumetric flux (ms^{-1})
p	pressure (Nm^{-2})
r	density ratio
u	velocity (ms^{-1})

Greek Letters

α	volume fraction
λ	wavelength (m)
ν	kinematic viscosity (m^2s^{-1})
ρ	density (kgm^{-3})
σ	surface tension (Nm^{-1})
ω	angular frequency (s^{-1})

Subscripts

1	liquid phase
2	vapour phase
i	interfacial
r	relative

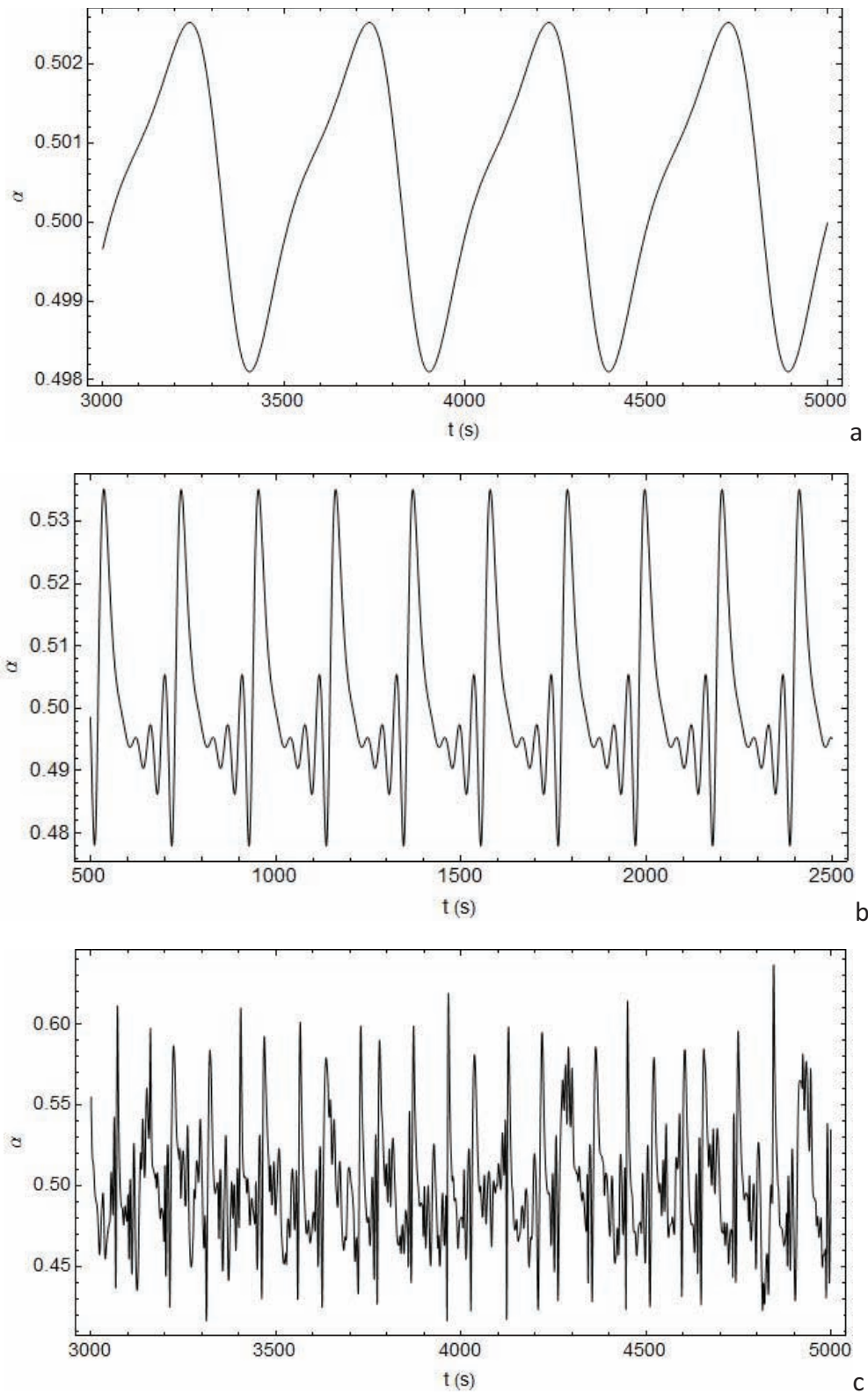


Figure 3

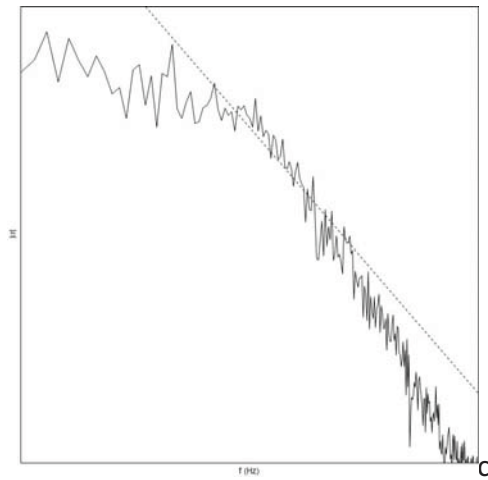
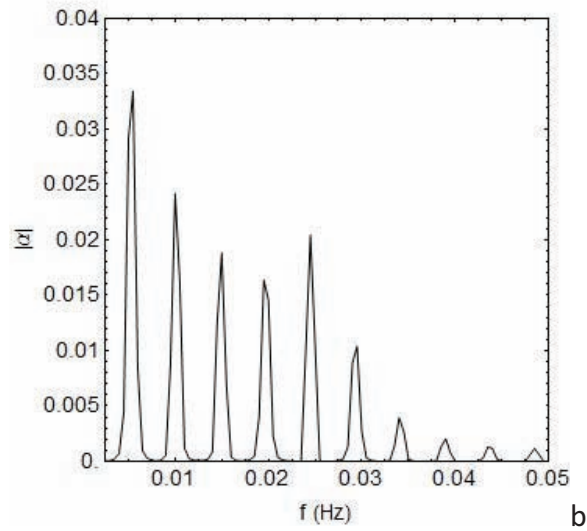
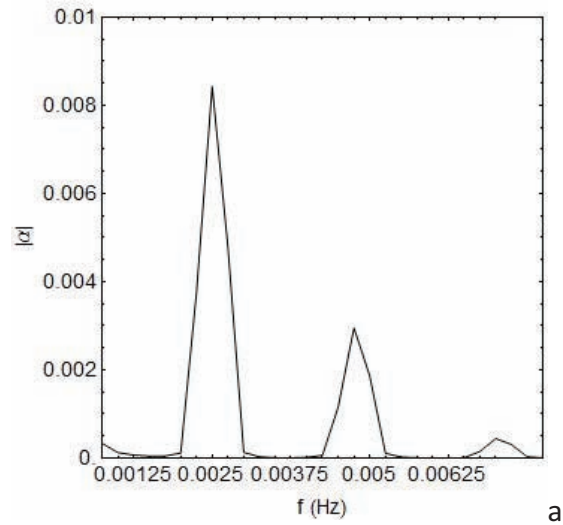


Figure 4